Hindawi Publishing Corporation
Mathematical Problems in Engineering
Volume 2016, Article ID 8216746, 8 pages
http://dx.doi.org/10.1155/2016/8216746

Research Article

Design and Evaluation for Target Indicated Torque Based Engine Starting Control Strategy in a High Pressure Common Rail Diesel Engine

Xuedong Lin, Xiaomei Han, and Degang Li

State Key Laboratory of Automobile Simulation and Control, Jilin University, Changchun 130022, China

Correspondence should be addressed to Degang Li; ldg@jlu.edu.cn

Received 16 November 2015; Accepted 17 February 2016

Academic Editor: Muhammad N. Akram

The diesel engine power demand of the start condition can be separated into two parts including resistance overcoming and acceleration realization for the reason that there is no power output during the starting process. The present paper mainly focuses on the fuel injection quantity control based on the engine power demand especially the acceleration demand for the resistance force is fixed for a specific engine, and the starting acceleration velocity is set as a target curve so that the acceleration process can also be fixed. The feasibility of the start control strategy proposed in this paper was verified by a comparison of the traditional starting control with a constant fuel quantity, and starting performance of the target acceleration based control shows predominance to the constant quantity control. And then the comparison between various starting acceleration processes, which was realized by the settings of acceleration curve slope factor, was conducted and results showed that the acceleration processes with higher slope factors perform better.

1. Introduction

Diesel engine is getting more and more popular for its efficiency and reliability [1] under the increasingly strict emission law and the low carbon demand [2, 3]. Misfire and low combustion efficiency always accompany diesel engine starting process [4, 5] for the high blow-by level, the low engine speed, and the low engine block temperature [6, 7]. As a result, emissions during the starting process, especially HC and CO emissions [8, 9], play an important role in the engine emission performance [10, 11]. And the diesel engine starting performance can be even poor, especially when it comes to the combustion efficiency [12], at the extremely low temperature [13, 14]. For the purpose of improving the diesel engine cold start performance, the heat assistance devices, mainly glow plug, are widely used. Researches concerning the ignition and in-cylinder combustion process of diesel engines fixed with glow plugs show that the well-calibrated multiple injection with the assistance of glow plug can improve the combustion process so that it shortens the starting time without much idle instability [15], and, with the assistance of high speed visualization in an optical engine, the pilot ignition is found to be occurring in the vicinity of the glow plug and strongly influence the main combustion initiation [16]; moreover, the spray-glow plug configuration can influence the equivalence ratio on glow plug vicinity so that ignition is influenced and the higher injection velocity and the lower injection mass per orifice can reduce the ignition probability, but the combustion rate increases when the injection momentum is higher, so a trade-off between ignition and combustion process has to be considered [17, 18]. Broatch et al. [19] proposed a new method for estimating the threshold temperature for self-ignition of fuel during cold start of diesel engines. They concluded that the threshold in-cylinder temperature was about 415°C for both low and high compression ratio engines and it could well instruct the application of glow plug under extremely low temperature. To satisfy the emissions demand reducing the NO_x and CO_2 emissions while keeping the CO, HC, and PM in control, lowering the engine compression ratio is a reasonable solution. The cold start problems of low compression ratio diesel engines are even more severe comparing the conventional compression ratio engines [20–24]. The hardware configuration, especially the spray-glow plug relative position, needs to be justified,

and the injection calibration is also needed to be optimized [21]. The pilot injection plays an important role in the ignition and combustion process [22–24] and the swirl number should be modified to the suitable level [20].

Comparing with the diesel engine starting at extremely low temperature, the starting at the normal temperature (around 30°C) is more frequently used. Peng et al. and Cui et al. researched influence of EGR on ignition and combustion during diesel engine starting at the normal environmental temperature which is common in south China; they found that the optimal opening of recirculation valves can advance the first firing cycle and reduce the duration of heavy smoke emission; it could be explained by the existence of reaction intermediates, such as ketohydroperoxides that could enhance the low temperature reaction, generated in the non-firing cycles [25, 26].

Most diesel engine starting concerning researches are focusing on the in-cylinder ignition and combustion, and, for the popularity and excellent performance of MAP based starting control (it means an array that the target value can be looked up by the relevant coordinates), few innovations on the starting process control have been proposed [27]. The present paper mainly focuses on the research on the diesel engine starting control that acceleration process defined before. The fuel quantity to be injected is calculated according to the real-time indicated torque which is acquired by an interpolation in a resistance torque MAP to get the resistance torque and a real-time calculation according to the acceleration curve defined before to get the acceleration torque. The starting control strategy proposed here can guarantee the accuracy of injection quantity according to the engine power demand, as well as the responsiveness of injection and engine speed control.

2. Methodology Description

For the reason that there is no power output during the engine starting-up process, the power generated by the fuel combustion is only separated into two parts: power for the engine resistance force and power for the engine acceleration. So the indicated torque of diesel engine starting process can be described as

$$\mathrm{Trq}_{i,\mathrm{start}} = \mathrm{Trq}_a + \mathrm{Trq}_r, \tag{1}$$

where $\mathrm{Trq}_{i,\mathrm{start}}$ is the indicated torque of the starting process, Trq_a is the torque for engine acceleration during the starting process, and Trq_r is the torque for overcoming the resistance force including the friction force and the requirement for necessary auxiliary devices.

For the reason that a well-performed starting process can be depicted as a shorter starting time, a smoother transition to the idle condition, and a lower emission level, an acceleration function is designed for the purpose of satisfying the above requirements as much as possible and the schematic diagram of the acceleration curve is depicted in Figure 1. The acceleration function is a segmented function that divides the starting acceleration curve into two parts—one presents a higher acceleration velocity to guarantee the engine speed

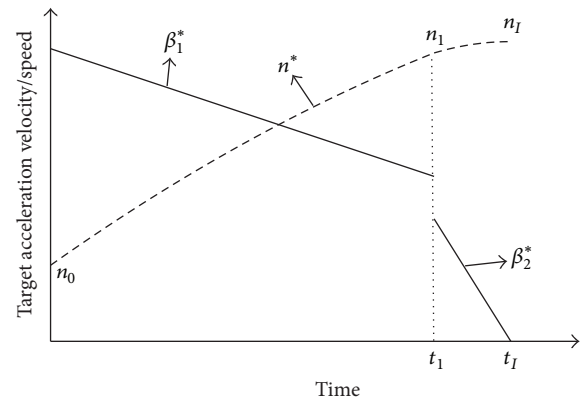

Figure 1: Schematic diagram of the target starting acceleration velocity curve.

ascend quickly and the other presents a lower acceleration velocity to acquire a smooth transition to idling. Both segments of the acceleration velocity curve are linear functions for the purpose of reducing the ECU calculated quantity and so improving the response performance of the ECU. The acceleration functions can be expressed as follows:

$$\beta_1^*(t) = \frac{(n_1 - n_0)\pi}{30t_1} + \frac{\pi k t}{30} - \frac{\pi k t_1}{60}, \quad t \in (0, t_1], \tag{2}$$

$$\beta_2^*(t) = \frac{\pi(n_1 - n_2)(t - t_1)}{15t_2^2} + \frac{\pi(n_2 - n_1)}{15t_2}, \quad t \in (t_1, t_I], \tag{3}$$

$$t_I = t_1 + t_2, \tag{4}$$

where t_1 is the time range for the first part acceleration velocity, t_2 is the time range for the second part acceleration velocity, t_I is the target start-up time, n_0 is the engine speed where fuel firstly started to be injected, n_1 is the target engine speed at the t_1 moment, and n_2 is the engine speed marking starting successfully. The independent variable t of the above equations is acquired by the internal timer of the ECU; it starts to count once the fuel is firstly injected and the update frequency of t is 1 ms.

Because the engine starting process is a transient condition, there are many uncertainties during the starting process and it is difficult to guarantee that the real engine operation agrees with the target acceleration curve. With the consideration of the above problems, a real-time correction strategy for the starting control is designed and the control flow diagram is presented in Figure 2.

The time counter in Figure 2 is equal to the independent variable t of the target acceleration velocity functions. When the time counter is less than t_1 but the engine speed is more than n_1, it means that the engine speed reaches the target value ahead of schedule; if the acceleration velocity keeps at the $\beta_1(t)$ function segment, the subsequent speed growth can be so violent that the speed overshoot will appear, and, for the purpose of solving the problem, the time counter is compulsively set to t_1 under this condition and the acceleration

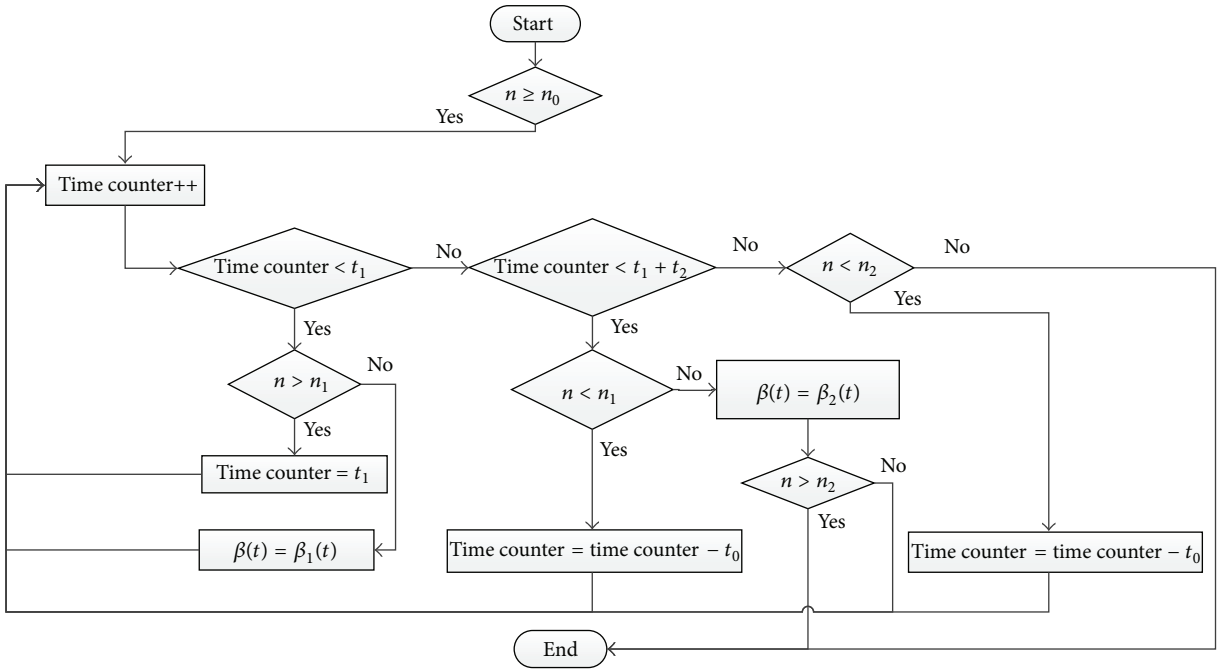

Figure 2: Flow diagram for starting control correction.

velocity turns to the $\beta_2(t)$ function segment where acceleration is much lower, so that a smooth starting to idling transition is secured. When the time counter is between t_1 and t_I but the engine speed is less than n_1, it can be inferred that the speed has not reached the anticipative value, so t_0 is subtracted from the time counter to make the time counter less than t_1 so that higher acceleration ($\beta_1(t)$) is supplied. When the time counter is larger than t_I but the engine has not reached n_2, it can be inferred that acceleration is still in need, so t_0 is subtracted from the time counter to make the time counter less than t_I and lower acceleration velocity is supplied to secure slow engine acceleration.

The starting acceleration torque can be demonstrated as follows:

$$\mathrm{Trq}_{a_1} = \frac{(n_1 - n_0)\pi I}{30t_1} + \frac{\pi I k t}{30} - \frac{\pi I k t_1}{60}, \quad t \in (0, t_1], \tag{5}$$

$$\mathrm{Trq}_{a_2} = \frac{\pi I (n_1 - n_2)(t - t_1)}{15t_2^2} + \frac{\pi I (n_2 - n_1)}{15t_2}, \quad t \in (t_1, t_I], \tag{6}$$

where I is the rotational inertia of the test engine.

The parameters including k, t_1, t_I, n_0, n_1, and n_2 are designed to be calibrating parameters and the adjustment of any of the above parameters will change the acceleration process.

The starting resistance torque (Trq_r) can be obtained by motoring tests, the MAP for resistance torque lookup is shown in Figure 3, and the real-time Trq_r is acquired by interpolation with the real-time engine speed and the coolant temperature acquired by corresponding sensors.

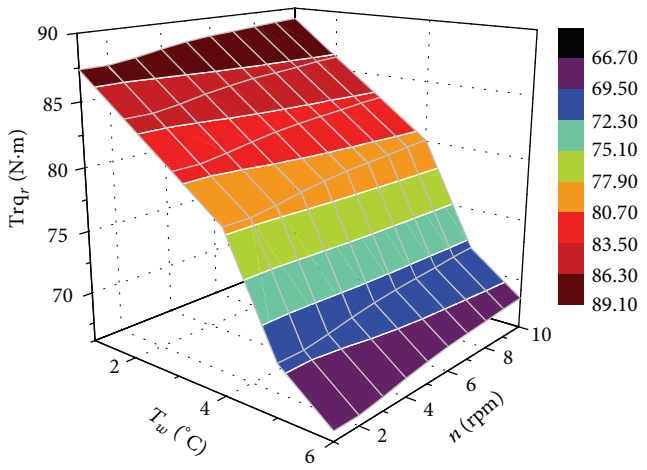

Figure 3: Starting resistance torque MAP.

As a result, the indicated torque $\mathrm{Trq}_{i,\mathrm{start}}$ is acquired after the obtainment of Trq_a and Trq_r so that the fuel quantity to be injected is confirmed with the indicated torque, and the torque to fuel transition process, which is referred to the Bosch EDC17 software documentation [28], will not be repeated here.

3. Experimental Setup and Procedure

3.1. Experimental Setup. The experiments were conducted on a four-cylinder high pressure common rail diesel engine. The open access ECU named HT5 is utilized in the research and the MCU module of the test ECU is a dual-core 16-bit high-performance MCU from the Freescale named MC9S12XEP10

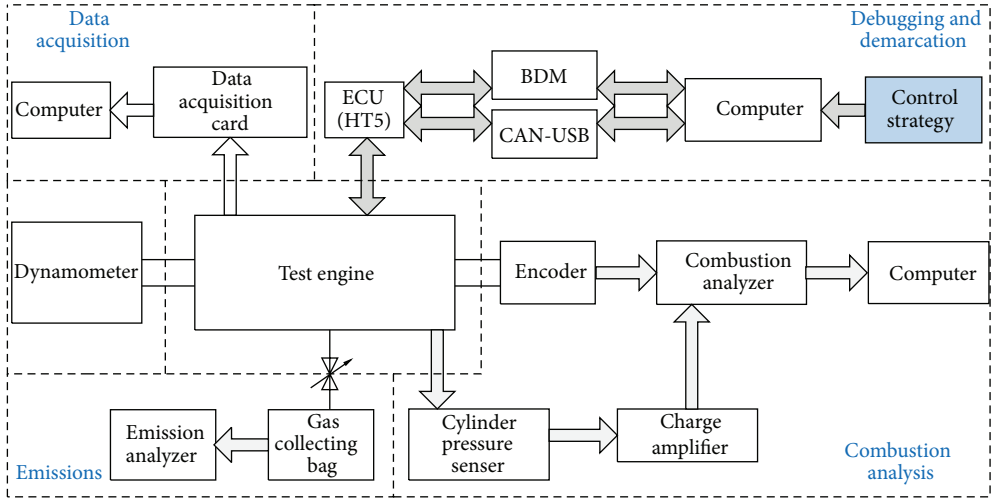

Figure 4: Test bench setup.

Table 1: Engine specification.

Description	Specification
Engine type	Four-stroke inline diesel engine
Air system	Turbocharged intercooled
Number of cylinders	4
Bore	93 mm
Stroke	102 mm
Compression ratio	17.2 : 1
Displacement volume	2.771 L
Rated power at speed	70 kW@3600 rpm
Maximum torque at speed	225 N·m@1600~2600 rpm
Minimum specific fuel consumption	≦218 g/kW·h
Common rail system	BOSCH 2nd generation HPCR system
Injector	Bosch CR 12.0

[29, 30], which consisted of modules including ATD, PIT, PWM, SPI, SCI, I/O, and CAN. The target acceleration (target indicated torque) based diesel engine starting control strategy is compiled with the Freescale CodeWarrior software and then loaded into the ECU. The real-time calibration and monitoring for the test engine can be realized by the HT-Link software which is designed for matching the HT5 ECU. Test engine specifications are given in Table 1.

Schematic of the experimental setup is shown in Figure 4. Cylinder pressure was measured by a piezoelectric pressure transducer (Kistler), which was fixed in the first cylinder and connected to a charge amplifier (Kistler), then finally to high speed combustion data acquisition and analysis system (ONOSOKKI). A magnetic valve connecting with a gas collecting bag was fixed in the exhaust manifold of the first cylinder and it only opened at the exhaust stroke of the first cylinder during the starting process for the purpose of collecting the first cylinder emissions of the starting condition.

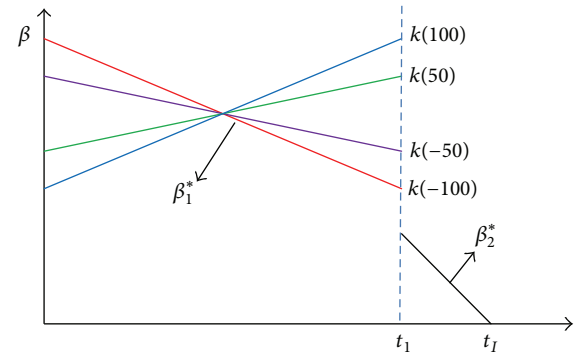

Figure 5: Schematic diagram of acceleration velocity curve with various slope factors.

An emission analyzer (HORIBA MEXA-7100DEGR) was used to measure CO, CO_2, HC, and NO_x in the exhaust.

3.2. Experimental Procedure. For the purpose of verifying the feasibility of the control strategy proposed in the present paper, a comparison between the traditional starting injection control that the injection quantity kept at a reasonable constant level (25 mg) and the target acceleration based starting injection control was conducted. And then, for the purpose of researching the influence of different acceleration process on the starting performance, starting with various acceleration curves was contrasted. Differences of the acceleration curves were realized by the calibration of the coefficient k (in (2) and (5)) representing the slope factor of the acceleration curve. The schematic diagram of acceleration velocity curve with various slope factors is shown in Figure 5.

During the experiment, coolant temperature was kept at 30°C. The pilot injection, injecting 10% of the whole fuel of each stroke at 18°CA before top dead center, was adopted, and the following main injection was injected at 6°CA before top dead center. The rail pressure was kept at 60 MPa. The fuel injection initiation symbol speed (n_0) was set to 200 rpm,

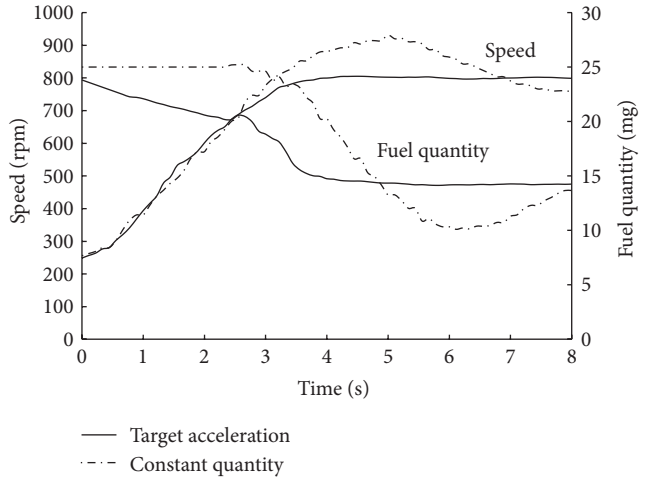

Figure 6: Speed comparison between different control strategies.

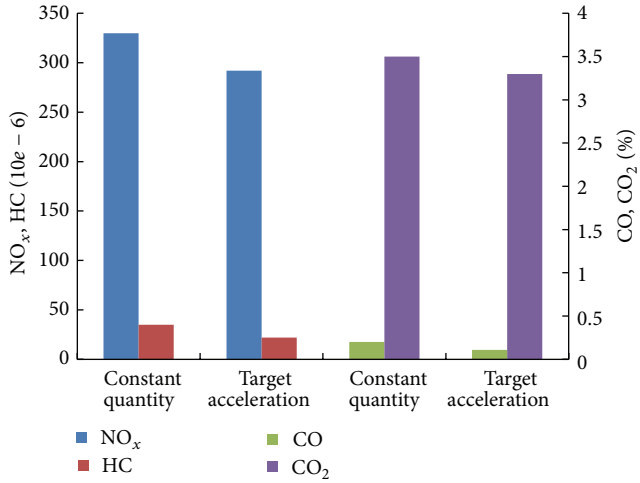

Figure 7: Emissions comparison between different control strategies.

speed symbolizing switch between the higher acceleration and the lower acceleration (n_1) was set to 760 rpm, and the successfully starting-up symbol speed (n_2) was set to 790 rpm. The target starting-up time t_I was set to 3 s and the duration for the quicker acceleration process (t_1) was set to 2.5 s.

4. Results and Discussion

Figure 6 presents the engine speed comparison between the target acceleration based control strategy (namely, target acceleration control in the following text) and the constant injection quantity starting control strategy (namely, constant quantity control in the following text). A great fluctuation of engine speed from the constant quantity control is displayed whereas the starting to idling transition is pretty smooth in the target acceleration control. The fuel quantity in the subsequent idle condition fluctuates much in the constant quantity control for the application of PID control but that in the target acceleration control keeps at a stable level because the fuel quantity injected is according to the engine operation demand strictly and little fuel quantity overshoot appears.

Figure 7 describes the emission characteristics from different control strategies. The emission performance of the target acceleration control shows predominance to the constant quantity control. The HC emission from the constant quantity control is 59% higher than that from the target acceleration control, the CO emission is 81.8% higher than target acceleration control, NO_x is 13% higher than target acceleration control, and CO_2 is 6% higher than the target acceleration control. The higher CO and HC emissions indicate that combustion efficiency of the constant quantity control is lower and the higher CO_2 and NO_x emissions mean that more fuel was consumed in the constant quantity control.

With the results derived from Figures 6 and 7, the practicability of the target acceleration based starting control strategy is well proved, so further researches were conducted.

The engine speeds of different acceleration curve slope factors are compared in Figure 8. All the four experimental

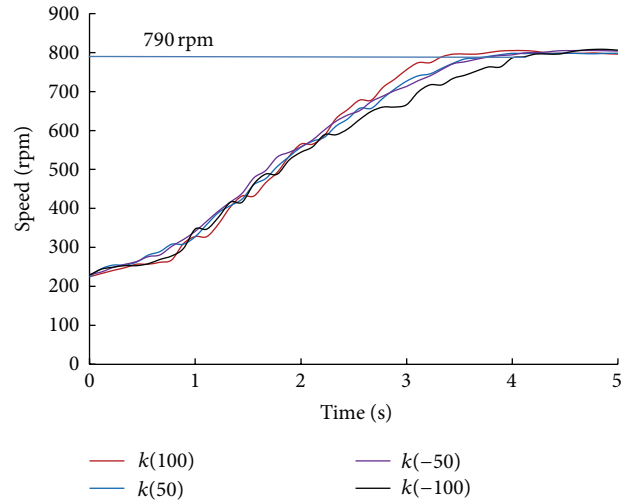

Figure 8: Engine speed of different slope factors.

settings present smooth start to idle transitions, but the variability in starting-up time appears. The shortest starting-up time is from $k(100)$ whereas the longest starting-up time is from $k(-100)$, a more visualized result that in form of cycle number is shown in Figure 9, where the higher slope factor (k) shows a lower starting-up cycle number. It can be inferred from Figure 8 that only when the engine speed is larger than 600 rpm, the difference between the influences of various slope factors on engine speed becomes obvious. It can be explained that when the engine speed is large enough, the in-cylinder fluid flow is strong enough to well promote air fuel mixing so that the difference in injection quantity becomes obvious.

Figure 10 shows the fuel quantity injected per stroke during the starting process by cycles. The first 8 cycles present the same trend with the curve in Figure 5, and from the ninth cycle on the fuel quantity fluctuation appears for the reason that t_1 time is arrived but the speed n_1 has not been reached,

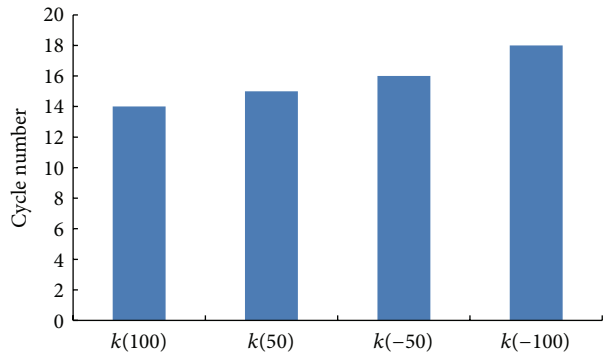

Figure 9: Starting cycles of different slope factors.

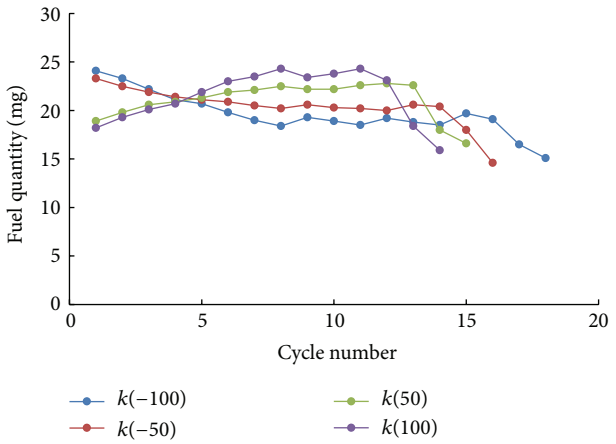

Figure 10: Engine speed and fuel injected per stroke by cycles.

so the time counter is minus by 500 ms and fuel quantity is back to the level at the corresponding time. The fuel quantity of the last two cycles of each experimental settings drops quickly for the reason that the slow acceleration stage is arrived.

The maximum in-cylinder pressure of the starting cycles (except the first cycle for the appearance of misfire) from different slope factor settings is shown in Figure 11, the agreement between the injection quantity and the maximum in-cylinder pressure is displayed, and the consistency between injection quantity and the maximum in-cylinder pressure gets more obvious from the ninth cycle. It can be a reasonable explanation for the phenomenon shown in Figure 8 that the engine speed variation of different slope factor settings becomes obvious when the engine speed is larger than 600 rpm.

The emission performance of different acceleration process is presented in Figure 12, the lowest HC emission is from $k(50)$, the HC emission of $k(100)$ is 5% higher than that of $k(50)$ and that of $k(-50)$ is 15% higher than $k(50)$, and the highest HC emission is from $k(-100)$, which is 25% higher than the lowest one. The CO emission of $k(100)$ and $k(50)$ is at the same level and that of $k(-50)$ and $k(-100)$ is 30% and 40% higher separately. The NO_x and CO_2 emissions show the reverse trend to the CO and HC emissions for the reason that

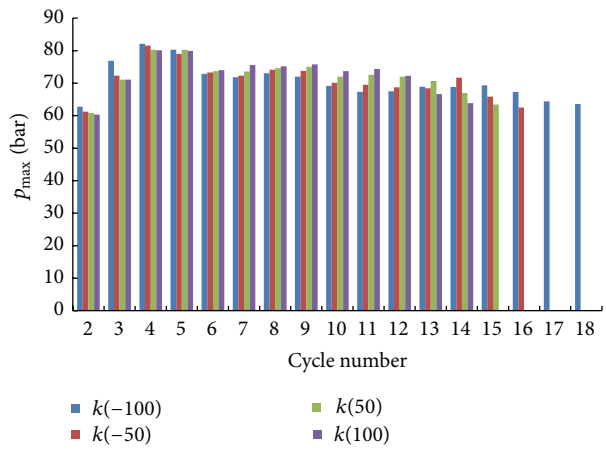

Figure 11: Maximum cylinder pressure of each starting cycle.

the lower HC and CO emissions signify the higher combustion efficiency as well as the higher combustion temperature which leads to the higher NO_x and CO_2 emissions. The highest NO_x emissions from $k(50)$ are 5.5% higher than the lowest one $k(-100)$, and the highest CO_2 emission from $k(50)$ is 9% higher than the lowest one $k(-100)$; it is not so obvious when comparing with the difference in HC and CO emissions.

With the consideration of both starting-up time and the emission performance, the acceleration curves with the higher slope factors ($k(100)$ and $k(50)$) perform better.

The most common diesel engine starting control strategy nowadays is the MAP based control that the fuel to be injected or the indicated torque of the starting condition is calibrated with plenty of tests aforehand; with the consideration of idle stability and the smooth start to idle transition, the fuel quantity tends to be descending with the increasing of engine speed, and it presents the same trend as the above-mentioned acceleration curve with the minus slope factors, so it can be concluded that the fuel quantity should increase with the increase of engine speed to a reasonable level and then decrease when the engine speed is near to the target idle speed to secure a smooth start to idle transition. The conclusion can be instructive for the diesel engine starting MAP calibration.

5. Conclusions

A novel diesel engine starting control strategy based on the target acceleration curve is proposed in the present paper. The fuel quantity injected per stroke is calculated according to the real-time acceleration velocity demand. Experiments include the comparison between different starting control strategies (target acceleration control and constant quantity control) and the comparison between different starting acceleration processes (different slope factor of the acceleration curve). The results are summarized as follows:

(1) A great fluctuation of engine speed in the constant quantity control is displayed whereas the starting to idling transition is pretty smooth in the target acceleration control. It can be explained that in the target acceleration control fuel injection quantity is

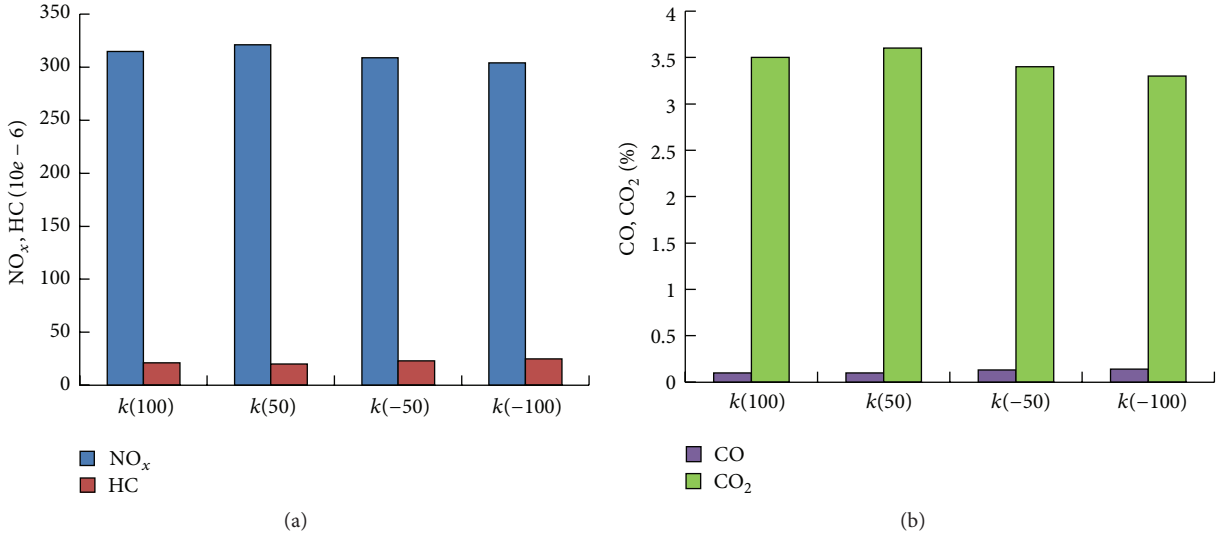

Figure 12: Emission comparison of different slope factors.

controlled by the real-time engine operation demand including the resistance force and the acceleration demand and almost no more fuel is injected beyond the requirement, but in the constant quantity control the fuel quantity is calibrated at a reasonable level by tests and experiences so that fuel quantity overshoot is unavoidable. The fuel injection performance can directly influence the emission performance, so the target acceleration control shows predominance to the constant quantity control when it comes to the engine emissions.

(2) The variation of the acceleration process is realized by the settings of acceleration curve slope factor and four different slope factors including $k(100)$, $k(50)$, $k(-50)$, and $k(-100)$ were experimentally compared. The different acceleration curve can influence the starting-up time and a higher slope factor of the acceleration curve presents a lower start-up cycle number; the influence of the difference of injection quantity caused by the settings of acceleration curve becomes obvious when the engine speed is larger than 600 rpm in the present research.

(3) The lowest HC emission is from $k(50)$, which is 25% lower than the highest one $k(-100)$, and that of $k(100)$ is 5% higher than $k(50)$; the CO emission of $k(50)$ and $k(100)$ is at the same level and 40% lower than the highest one $k(-100)$. The NO_x and CO_2 emissions show the reverse trend to the CO and HC emissions. The highest NO_x emissions from $k(50)$ are 5.5% higher than the lowest one $k(-100)$ and that of $k(100)$ is 1.9% lower than $k(50)$; the highest CO_2 emission from $k(50)$ is 9% higher than the lowest one $k(-100)$ and that of $k(100)$ is 2.8% lower than $k(50)$.

(4) With comprehensive consideration of the starting performance, the starting acceleration curves with the higher slope factors perform better, which means that the rising first and falling later injection quantity trend during the diesel engine starting process is more reasonable, and the conclusion can be instructive for the widely used diesel engine starting MAP calibration process.

Conflict of Interests

The authors declare that there is no conflict of interests regarding the publication of this paper.

Acknowledgments

This work was financially supported by the Natural Science Foundation of Jilin Province (3D515U172415) and Industrial Technology Development Project of Jilin Province Development and Reform Commission (2014Y093) and Scientific and Technological Developing Scheme of Ji Lin Province (20150101032JC).

References

[1] J. B. Heywood, *Internal Combustion Engine Fundamentals*, McGraw-Hill, New York, NY, USA, 1988.

[2] G. D. Neely, D. Mehta, and J. Sarlashkar, "Diesel cold-start emission control research for 2015–2025 LEV III emissions-part 2," SAE Paper 2014-01-1552, 2014.

[3] M. Weilenmann, J.-Y. Favez, and R. Alvarez, "Cold-start emissions of modern passenger cars at different low ambient temperatures and their evolution over vehicle legislation categories," *Atmospheric Environment*, vol. 43, no. 15, pp. 2419–2429, 2009.

[4] A. Manuel, D. Gonzalez, G. L. Borman, and R. D. Reitz, "A study of diesel cold starting using both cycle analysis and multidimensional calculations," SAE Paper 910180, SAE International, 1991.

[5] A. Zahdeh and N. Henein, "Diesel cold starting: actual cycle analysis under border-line conditions," SAE Paper 900441, 1990.

[6] Z. Han, N. Henein, and B. Nitu, "Diesel engine cold start combustion instability and control strategy," SAE Paper 2001-01-1237, 2001.

[7] N. A. Henein, A. R. Zahdeh, and M. K. Yassine, "Diesel engine cold starting: combustion instability," SAE Paper 920005, SAE International, 1992.

[8] C. Dardiotis, G. Martini, A. Marotta, and U. Manfredi, "Low-temperature cold-start gaseous emissions of late technology passenger cars," *Applied Energy*, vol. 111, pp. 468–478, 2013.

[9] J. Windeatt, G. Brady, P. Usher, H. Li, and A. Hadavi, "Real world cold start emissions from a diesel vehicle," SAE Paper 2012-01-1075, 2012.

[10] P. Bielaczyc, J. Merkisz, and J. Pielecha, "A method of reducing the exhaust emissions from DI diesel engines by the introduction of a fuel cut off system during cold start," SAE Paper 2001-01-3283, SAE International, 2001.

[11] A. Broatch, J. M. Luján, S. Ruiz, and P. Olmeda, "Measurement of hydrocarbon and carbon monoxide emissions during the starting of automotive di Diesel engines," *International Journal of Automotive Technology*, vol. 9, no. 2, pp. 129–140, 2008.

[12] A. Roberts, R. Brooks, and P. Shipway, "Internal combustion engine cold-start efficiency: a review of the problem, causes and potential solutions," *Energy Conversion and Management*, vol. 82, pp. 327–350, 2014.

[13] L. Zhong, S. Gruenewald, and N. A. Henein, "Lower temperature limits for cold starting of diesel engine with a common rail fuel injection system," SAE Paper 2007-01-0934, 2007.

[14] R. A. Sakunthalai, H. Xu, D. Liu, J. Tian, M. Wyszynski, and J. Piaszyk, "Impact of cold ambient conditions on cold start and idle emissions from diesel engines," SAE Paper 2014-01-2715, SAE International, 2014.

[15] D. John, P. Ghodke, N. Gajarlawar, and J. J. lng, "Experiences in cold start optimization of a multi-purpose vehicle equipped with 2.2L common rail diesel engine," SAE Paper 2011-01-0124, 2011.

[16] J. V. Pastor, J. M. García-Oliver, J. M. Pastor, and J. G. Ramírez-Hernández, "Ignition and combustion development for high speed direct injection diesel engines under low temperature cold start conditions," *Fuel*, vol. 90, no. 4, pp. 1556–1566, 2011.

[17] J. M. Desantes, J. M. García-Oliver, J. M. Pastor, and J. G. Ramírez-Hernández, "Influence of nozzle geometry on ignition and combustion for high-speed direct injection diesel engines under cold start conditions," *Fuel*, vol. 90, no. 11, pp. 3359–3368, 2011.

[18] J. V. Pastor, V. Bermúdez, J. M. García-Oliver, and J. G. Ramírez-Hernández, "Influence of spray-glow plug configuration on cold start combustion for high-speed direct injection diesel engines," *Energy*, vol. 36, no. 9, pp. 5486–5496, 2011.

[19] A. Broatch, S. Ruiz, X. Margot, and A. Gil, "Methodology to estimate the threshold in-cylinder temperature for self-ignition of fuel during cold start of Diesel engines," *Energy*, vol. 35, no. 5, pp. 2251–2260, 2010.

[20] H. Perrin, J.-P. Dumas, O. Laget, and B. Walter, "Analysis of combustion process in cold operation with a low compression ratio diesel engine," SAE Paper 2010-01-1267, SAE International, 2010.

[21] B. Walter, H. Perrin, J. P. Dumas, and O. Laget, "Cold operation with optical and numerical investigations on a low compression ratio diesel engine," SAE Paper 2009-01-2714, SAE International, 2009.

[22] P. Pacaud, H. Perrin, and O. Laget, "Cold start on diesel engine: is low compression ratio compatible with cold start requirements?" SAE Paper 2008-01-1310, SAE International, 2008.

[23] O. Laget, P. Pacaud, and H. Perrin, "Cold start on low compression ratio diesel engine: experimental and 3D RANS computation investigations," *Oil & Gas Science and Technology—Revue d'IFP Energies nouvelles*, vol. 64, no. 3, pp. 407–429, 2009.

[24] D. MacMillan, A. La Rocca, and P. J. Shayler, "The effect of reducing compression ratio on the work output and heat release characteristics of a DI diesel under cold start conditions," SAE Paper 2008-01-1306, SAE International, 2008.

[25] H. Peng, Y. Cui, L. Shi, and K. Deng, "Effects of exhaust gas recirculation (EGR) on combustion and emissions during cold start of direct injection (DI) diesel engine," *Energy*, vol. 33, no. 3, pp. 471–479, 2008.

[26] Y. Cui, H. Peng, K. Deng, and L. Shi, "The effects of unburned hydrocarbon recirculation on ignition and combustion during diesel engine cold starts," *Energy*, vol. 64, pp. 323–329, 2014.

[27] Y. Huang, F. Yang, M. Ouyang, L. Chen, and X. Yang, "Optimal feedback control with in-cylinder pressure sensor under engine start conditions," SAE Paper 2011-01-1422, 2011.

[28] Bosch, "The 3rd generation Common Rail from Bosch[R/OL]," December 2003, http://www.boschautoparts.co.uk/.

[29] Freescale, "MC9S12XEP100 Reference Manual Covers MC9S12XE Family, Rev. 1.15," 2008, http://www.freescale.com/.

[30] Freescale, CodeWarrior Development Tools, http://www.freescale.com.